*Engineering Fracture Mechanics* Vol. 23, No. 1, pp. 119–129, 1986
Printed in Great Britain.

0013-7944/86 $3.00 + .00
Pergamon Press Ltd.

# ANALYSIS OF HIGH-STRAIN-RATE ELASTIC–PLASTIC CRACK GROWTH

L. B. FREUND
Division of Engineering, Brown University, Providence, RI 02912, U.S.A.

J. W. HUTCHINSON
Division of Applied Sciences, Harvard University, Cambridge, MA 02138, U.S.A.

and

P. S. LAM
Division of Engineering, Brown University, Providence, RI 02912, U.S.A.

**Abstract**—For crack-tip speeds which are even a modest fraction of the lowest elastic wave speed of a material, the strain rates that are induced at material points close to the crack tip are enormous. Experimental evidence is available which suggests that the flow stress is a fairly strong function of plastic strain rate at the rates anticipated. An approximate analysis of the high-strain-rate crack-growth process has been developed on the basis of this observation, which is interpreted as implying that the elastic strain rates dominate the plastic strain rates. The features of the approximate analysis are reviewed, and the results of more recent complete numerical analysis of the same crack-growth model are described. Using the growth of a macroscopic cleavage crack in mild steel as a vehicle for discussing the model, it is found that the approximate model appears to capture the essence of the process for those temperatures at which cleavage crack growth is supported. The numerical results indicate deficiencies in the approximate analysis for higher temperatures.

## 1. INTRODUCTION

THE PHENOMENON under study is high-strain-rate crack growth as it occurs, for example, in structural steels. It is well known that such materials may or may not experience rapid crack growth in a predominantly cleavage mode, depending on the state of stress, the temperature, and the rate of deformation. Evidence on the influence of stress state and temperature is abundant in the technical literature, and data on the influence of loading rate on the variation of fracture toughness with testing temperature for two carbon steels have been reported recently by Wilson *et al.*[1]. It was found, for example, that an increase in loading rate as measured by average stress-intensity factor rate from $\dot{K}_I = 1\text{MPa}\cdot\text{m}^{1/2}/\text{s}$ to $\dot{K}_I = 2 \times 10^6\ \text{MPa}\cdot\text{m}^{1/2}/\text{s}$ resulted in an increase of more than 125°C in the cleavage transition temperature for a 1018 cold-rolled steel.

The physical processes which underlie the growth of cleavage cracks in steels have been of interest for many years. A particularly interesting qualitative discussion of the cleavage process in metals was presented by Stroh[[2], who exhibited remarkable insight into the process in view of the stage of development of fracture mechanics at the time.

The purpose here is to focus on the mechanics of rapid growth of a sharp macroscopic crack in an elastic–viscoplastic material which exhibits a fairly strong variation of flow stress with strain rate, particularly at very high strain rates. The general features of the process as "seen" by a material particle on or near the fracture path are straightforward. As the edge of a growing crack approaches a material particle, the stress magnitude tends to increase there due to the stress-concentrating effect of the crack edge. The material responds by flowing at a rate related to the stress level in order to mitigate the influence of the crack edge. It seems that the essence of cleavage is the ability to elevate the local stress to a critical level *before* plastic flow can accumulate to dilute the influence of the crack tip.

The problem was studied from this point of view by Freund and Hutchinson[3], who extracted conditions necessary for a crack to run a high velocity in terms of constitutive properties of the material, the rate of crack growth, and the overall crack-driving force. The model developed by [3] is briefly described here and some conclusions drawn on the basis of an approximate analysis are summarized. More recently, numerical calculations based on the same model have been carried out in order to develop some understanding of the range of validity

of certain assumptions made in the analysis, and the results of these calculations are reported here. In all cases, the growth of a plane-strain crack in the tensile opening mode is considered, and the small-strain description of deformation fields is employed.

An estimate of the plastic strain rate near the crack tip may be obtained to support the view that the actual strain rates are indeed very large. Suppose that the yield stress in shear of the material is $\tau_y$ and the elastic shear modulus is $\mu$. A *representative plastic strain rate* in the active plastic zone of maximum extent $R$ from a crack tip which is moving at speed $v$ is then taken to be the shear yield strain $\tau_y/\mu$ divided by the time required for the crack tip to travel the distance $R$ at speed $v$. Furthermore, under small-scale yielding conditions with remote energy release rate $G$, the maximum extent of the plastic zone is approximately $R \approx 0.14\mu G/\tau_y^2$. Consequently, an estimate of this representative plastic strain rate is

$$(\dot{\gamma}^p)_{est} \approx 7v\tau_y^3/\mu^2 G. \tag{1.1}$$

For a pure-cleavage crack in an iron single crystal, $G \approx 14$ J/m$^2$. Using typical values of $\mu$ and $\tau_y$, and taking $v$ to be one-tenth of the Rayleigh wave speed, the estimate (1.1) leads to values of $(\dot{\gamma}^p)_{est}$ between $10^6 s^{-1}$ and $10^7 s^{-1}$. Even for a macroscopic cleavage crack where $G$ might be 100 times larger than the value for pure cleavage, the estimated strain rates are still very large. Because of the nonuniformity of crack-tip fields, of course, point values of strain rate much larger than the estimate could be anticipated. Material rate effects, on the other hand, would tend to lower plastic strain rates.

## 2. THE MATERIAL MODEL

Experiments have been reported on the high-strain-rate response of materials, usually under more-or-less homogeneous states of deformation, and constitutive equations have been proposed. For absolute temperatures well below the melting temperature, it appears that the high-strain-rate response of iron may be divided into two regimes. These will be described first for states of homogeneous shear, and then generalized for a continuum-field formulation.

For strain rates above a certain level, hearafter called the *transition strain rate* $\dot{\gamma}_t$, the resistance to dislocation glide is essentially linear viscous resistance. If plastic flow is due primarily to dislocation motion, then the plastic strain rate may depend on flow stress $\tau$ according to

$$\dot{\gamma}^p = \dot{\gamma}_t + \dot{\gamma}_o(\tau - \tau_t)/\mu \qquad \text{for } \tau \geq \tau_t, \tag{2.1}$$

where $\tau_t$ is the value of $\tau$ when $\dot{\gamma}^p = \dot{\gamma}_t$. This form is suggested by the data on mild steel reported by Campbell and Ferguson[4], who give $\dot{\gamma}_t = 5 \times 10^3 s^{-1}$ and $\dot{\gamma}_o = 3 \times 10^7 s^{-1}$.

For plastic strain rates below the transition rate, the dependence on flow stress is not nearly as strong. The underlying mechanism appears to be thermally activated dislocation glide, and Frost and Ashby[5] propose a constitutive equation of the form

$$\dot{\gamma}^p = c_p \left(\frac{\tau}{\mu}\right)^2 \exp\left[-\frac{\Delta F_p}{kT}\left(1 - \left(\frac{\tau}{\tilde{\tau}}\right)^{3/4}\right)^{4/3}\right] \qquad \text{for } \tau \leq \tau_t, \tag{2.2}$$

where $\tilde{\tau}$ is the flow stress at 0 K. The values of all parameters appearing in (2.2) are given by Frost and Ashby, and complete stress–strain relations for four temperatures are presented graphically in [3]. Implicit in (2.1) and (2.2) is an assumption that plastic flow occurs predominantly by dislocation glide. If dislocation multiplication/generation contributes significantly to plastic flow, a weaker dependence of flow stress on plastic strain rate is anticipated (cf. Clifton[6]).

To generalize the constitutive equations to provide suitable field equations for continuum analysis, let $\dot{\gamma}^p = F(\tau)$ represent either (2.1) or (2.2), depending on the magnitude of $\tau$. Then the multiaxial plastic strain rate is taken to be

$$\dot{\epsilon}_{ij}^p = \tfrac{1}{2}F(\tau)\frac{s_{ij}}{\tau}, \tag{2.3}$$

where $s_{ij}$ is the stress deviator and $\tau = \sqrt{s_{ij}s_{ij}/2}$. In elastically deforming regions, elastic strain rate is related to stress $\sigma_{ij}$ by

$$\dot{\epsilon}^{e}_{ij} = \frac{1 + \nu}{E}\dot{\sigma}_{ij} - \frac{\nu}{E}\dot{\sigma}_{kk}\delta_{ij} \tag{2.4}$$

where $E$ is Young's modulus and $\nu$ is Poisson's ratio of the (assumed elastically isotropic) material. The relation applies when $\tau \leq \tau_y$. It is more convenient to view $\tau_y$ as the stress magnitude when the plastic strain rate falls to 1 $s^{-1}$ rather than a yield stress in the usual sense, and it is concluded from the analysis that the difference in viewpoint is immaterial.

## 3. STEADY CRACK GROWTH

Suppose that a crack has grown at speed $v$ for a time long enough to establish a steady mechanical state; that is, an observer travelling with the crack tip sees no variation in the mechanical fields. Further, suppose that the active plastic zone is completely surrounded by a well-defined elastic stress-intensity-factor field. Under these conditions, the time rate of change of any field quantity may be replaced by a spatial gradient in the direction of crack growth, and the influence of the applied loading is completely represented by the value of the dynamic stress-intensity factor $K$ or, equivalently, the value of the dynamic energy release rate $G$. The features of the model are more fully developed in [3].

The stress state for points very far from the crack tip is given by

$$\sigma_{ij} \approx \frac{K}{\sqrt{2\pi r}}\Sigma_{ij}(\theta, m) \tag{3.1}$$

as the radial distance $r$ from the crack tip becomes very large, where $m = v/c_R$, $c_R$ is the elastic Rayleigh wave speed of the material and $\Sigma_{ij}$ is the universal function of angle $\theta$ measured with respect to the crack plane (cf. Rice[7], Freund[8]). For points very close to the crack tip, it is assumed that the relationship (2.1) holds. If the stress is singular there, it can readily be shown that the elastic strain rates dominate the plastic strain rates, which implies immediately that

$$\sigma_{ij} \approx \frac{K_{tip}}{\sqrt{2\pi r}}\Sigma_{ij}(\theta, m) \qquad \text{as } r \to 0, \tag{3.2}$$

where $K_{tip}$ is a different, local stress-intensity factor. The fact that a material described by (2.1) can indeed support a square-root singular stress field has been noted by Lo[9] and Brickstad[10], and the latter used a similar result to advantage in numerical analysis of crack-growth phenomena. It should be noted that the inverse square-root dependence of $\sigma_{ij}$ on $r$ does not require that the plastic strain rate depends *linearly* on stress as in (2.1). The same singularity in stress will exist for any material for which $\dot{\gamma}^p$ is proportional to $(\tau - \tau_t)^q$ with $q < 3$. Consequently, the conclusions drawn on the basis of the linear relationship (2.1) are actually applicable for a range of viscoplastic material response.

The stress-intensity factor at the crack tip $K_{tip}$ is different from the remote $K$ because processes at the crack tip are "screened" from the remote loads by the intervening plastic deformation. The viewpoint was adopted in [3] that crack growth is controlled by the value of $K_{tip}$, and the objective of the analysis was to relate $K_{tip}$ to $K$. It was found to be advantageous to work in terms of energy variations. Consequently, the dynamic energy release rate $G$ is introduced. $G$ is related to stress-intensity factor $K$ through a generalization of Irwin's relationship by

$$G = f(m)\frac{1 - \nu^2}{E}K^2, \tag{3.3}$$

where $f(m)$ is a dimensionless function of crack-tip speed. $G$ represents the energy flow into

the crack-tip region per unit crack advance. An equivalent expression relates the near-tip stress-intensity factor $K_{tip}$ to the crack-tip energy release rate $G_{tip}$. The quantity $G_{tip}$ represents the energy released from the body per unit crack advance.

The matter of relating $G$ to $G_{tip}$ is pursued in [3] by enforcing an overall energy-rate balance by means of a particular path-independent integral. The balance is included here in the form

$$G_{tip} = G\frac{1}{V}\int_A \sigma_{ij}\dot{\epsilon}^p_{ij}\,dA - \int_{-h}^{h} U_e^*\,dh, \tag{3.4}$$

where $A$ is the area of the active plastic zone in the plane of deformation, $h$ is the thickness of the plastic wake far behind the crack tip, and $U_e^*$ is the residual elastic strain energy per unit crack advance stored in the remote wake. Equation (3.4) simply states that the energy being released from the body equals the energy flowing into the crack-tip region reduced by the energy being dissipated through active plastic flow, and further reduced by the energy being locked into the wake due to incompatible plastic strains. The expression in (3.4) is exact.

To make further progress analytically, it was found necessary to invoke certain assumptions, and these are briefly restated here. First, it can be estimated from the work of Dean and Hutchinson[11] that the elastic energy trapped in the wake region accounts for less than 10% of the energy flowing into the crack-tip region for steady crack growth in rate-independent elastic–plastic materials. The percentage is expected to be less here because only relatively small plastic strains are accumulated. For this reason, the last term in (3.4) was ignored. Next, to estimate the work dissipated through plastic flow in the active plastic zone, it was assumed that the stress distribution is given by (3.2) *everywhere* in the active plastic zone. Strictly speaking, this distribution is correct only asymptotically as $r \to 0$. In any case, with the stress distribution specified, the plastic strain distribution is given by (2.3), and the integral over $A$ may be evaluated. Finally, if the criterion for the crack to run under steady-state conditions is $G_{tip} = G^c_{tip}$, where $G^c_{tip}$ is a material specific value, then (3.4) reduces to the remarkably simple form

$$\frac{G}{G^c_{tip}} = 1 + D(m)P_c, \tag{3.5}$$

where $P_c$ is the dimensionless combination of mass density $\rho$ and other material parameters:

$$P_c = \frac{\dot{\gamma}_0\sqrt{\mu\rho}G^c_{tip}}{3\tau_t^2}\left[1 + \frac{2\dot{\gamma}_t\mu}{\dot{\gamma}_0\tau_t}\right], \tag{3.6}$$

and $D(m)$ is a function of crack-tip speed and, implicitly, of the Poisson ratio of the material. $P_c$ appears to be a monotonically increasing function of temperature for mild steel, and its value was estimated to be 0.6, 1.8, 3.4 and 6.4 for absolute temperatures of 0, 100, 200 and 300 K, respectively. The function $D(m)$ varies smoothly with crack speed; it has a minimum value of 0.109 at $m = 0.55$, and it is asymptotically unbounded as $m \to 0$ or $m \to 1$. A graph of $D(m)$ is shown in Fig. 1.

For a given value of $P_c$, the curve in Fig. 1 represents the variation of $G/G^c_{tip}$ with $m$. Assuming that the steady-state solutions are approximately valid under nonsteady conditions, the result suggests that a running crack nucleated under combinations of $G$ and $m$ lying below the contour will decelerate until either a solution state is reached or the crack arrests. Likewise, if nucleated with a combination lying above the contour, the crack will accelerate toward a solution on the branch of the curve with $m > 0.55$. The result in Fig. 1 is shown in [3] as a family of curves, each for a different value of $P_c$. The results may also be restated in terms of an *applied energy release rate* $G_s$ which has a more direct relationship to the applied loads than does $G$. The two quantities are related by $G = (1 - m)G_s$ for a half-plane crack in an otherwise unbounded solid, and this relationship appears to have broader applicability unless stress-wave effects are significant.

Two dimensionless parameters arise naturally in the analysis; these are denoted by $\alpha$ and

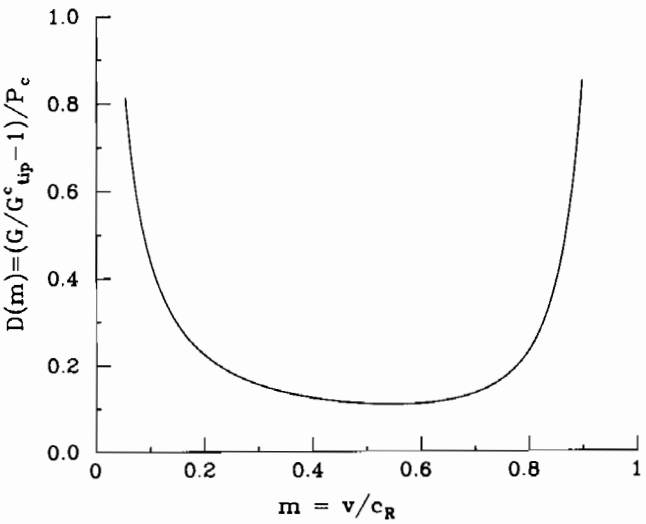


Fig. 1. A graph of the function $D$ in (3.5) *vs* crack-tip speed normalized by the Rayleigh wave speed for a Poisson ratio of 0.29.

$\beta$, and they are defined by

$$\alpha = \frac{\dot{\gamma}_t \mu^2 G}{\nu \tau_y^3}, \qquad \beta = \frac{\dot{\gamma}_0 \mu G}{\nu \tau_t^2}. \tag{3.7}$$

The parameter $\alpha$ is a measure of the plastic-strain-rate magnitude compared to a material time constant. In this sense, it is an absolute measure of strain rate for the process, which can be viewed as a high-rate process only if $\alpha$ is sufficiently small. The parameter $\beta$, on the other hand, is essentially a measure of plastic strain rate compared to the elastic strain rate. It is a relative measure of strain rate, and the approximate solution in [3] is valid only if $\beta$ is sufficiently small. Indeed, it is shown in [3] that not only is the estimate of energy release rate $G$ exact as $\beta \to 0$, but the rate of change $dG/d\beta$ is also exact as $\beta \to 0$.

To gain further insight into the range of validity of the approximate solution in [3], a full numerical analysis of the *same* steady growth problem was undertaken. The features of the computational procedure and the principal results are summarized next.

## 4. COMPUTATIONAL PROCEDURE

A finite-element mesh is fixed with respect to the moving crack tip and the governing equations are solved numerically with reference to this mesh. The geometry of the mesh, the relative sizes of the elements, the type of elements, and so on are the same as were used by Lam and Freund[12] in a study of steady growth of a tensile crack in a rate-independent elastic–plastic material. It is important that the outer boundary of the mesh be far from the crack tip compared to the maximum extent of the active plastic zone so that the use of the elastodynamic crack-tip solution as a boundary condition is legitimate. Some focussing of the mesh at the crack tip is also required so that the smallest elements at the tip are much smaller than the extent of the active plastic zone.

A rectangular coordinate system $(x_1, x_2, x_3)$ is introduced so that the $x_3$ axis coincides with the crack edge and the $x_1$ direction is the direction of crack growth. The deformation is plane strain, and is independent of $x_3$. It was found to be convenient to rescale the physical coordinates by the length parameter $l = \mu G/\tau_t^2$. The normalized coordinates are then denoted by superposed carets; that is, $\hat{x}_i = x_i/l$. Normalized components of stress, strain and displacement are also introduced; these too are denoted by superposed carets and are defined by

$$\hat{\sigma}_{ij} = \sigma_{ij}/\tau_t, \qquad \hat{\epsilon}_{ij} = \mu \epsilon_{ij}/\tau_t, \qquad \hat{u}_i = \mu u_i/\tau_t l. \tag{4.1}$$

The global equation which underlies the finite-element formulation is obtained by forming the inner product of a kinematically admissible, but otherwise arbitrary, displacement field $\delta u_i$ with the momentum equation, which in nondimensional form is

$$\frac{\partial \hat{\sigma}_{ij}}{\partial \hat{x}_j} = m_s^2 \frac{\partial^2 \hat{u}_i}{\partial \hat{x}_1^2}, \tag{4.2}$$

where $m_s = v/c_s$, and then integrating over the region of the body, say $R$, covered with the element array. The result is

$$\int_R \left( \delta\hat{\epsilon}_{ij} \hat{C}_{ijkl} \hat{\epsilon}_{kl} - m_s^2 \frac{\partial \delta \hat{u}_i}{\partial \hat{x}_1} \frac{\partial \hat{u}_i}{\partial \hat{x}_1} \right) \mathrm{d}R = \int_\Gamma \left( \delta\hat{u}_i \hat{\sigma}_{ij} n_j - m_s^2 \, \delta\hat{u}_i \frac{\partial \hat{u}_i}{\partial \hat{x}_1} n_1 \right) \mathrm{d}\Gamma + \int_R \delta\hat{\epsilon}_{ij} \hat{C}_{ijkl} \hat{\epsilon}_{kl}^{\mathrm{p}} \, \mathrm{d}R; \tag{4.3}$$

$\Gamma$ is the boundary of $R$, $n_i$ is the outward normal to $\Gamma$, and $\hat{C}_{ijkl}$ is the positive definite elasticity tensor normalized by the shear modulus $\mu$. It is assumed in writing (4.3) that the total strain is the sum of the elastic strain and the plastic strain.

The basic idea of the numerical algorithm for integrating the equations of motion stems from the work of Dean and Hutchison[11] and Parks, Lam and McMeeking[13]. The unknown plastic strain appears as a body force term on the right side of (4.3). Consequently, the procedure starts with $\hat{\epsilon}_{ij}^{\mathrm{p}} = 0$ and with a known elastic-stress distribution. The plastic strain at any point is estimated by integrating the incremental stress–strain relations along the forward pathline of the point, and (4.3) is solved by the finite-element method to obtain a new estimate of stress. These steps are repeated iteratively until a convergence criterion is satisfied. Because earlier work dealt with rate-independent material models, it was necessary to derive a finite-difference integration formula which was suitable for the constitutive equation used to model the rate-sensitive material. This derivation was based on the tangent modulus method of Peirce, Shih and Needleman[14].

The constitutive equations (2.3, 4) can be inverted to yield the deviatoric stress rate $\dot{s}_{ij}$ in terms of the deviatoric stress and the deviatoric strain rate $\dot{e}_{ij}$:

$$\dot{s}_{ij} = 2\mu \left[ \dot{\mathrm{e}}_{ij} - \frac{1}{2} F(\tau) \frac{s_{ij}}{\tau} \right]. \tag{4.4}$$

If the incremental form of (4.4) is incorporated directly into a finite-element formulation, it leads to an explicit Euler time-integration scheme in which the finite-element stiffness matrix is derived from the elastic stiffnesses. In some circumstances this approach requires extremely small time steps in order to ensure numerical stability. Peirce, Shih and Needleman[14] introduced an estimate of the change in the second term in (4.4) during the current time increment to yield a tangent stiffness which depends on the magnitude of the time step and on the material properties. The modified tangent stiffness is considerably reduced from the elastic stiffness, and it leads to improved numerical stability[14].

For the steady-growth problem at hand, eqn (3.8) of [14] reduces to the nondimensional form

$$\Delta \hat{s}_{ij} = 2 \left[ \Delta \hat{e}_{ij} - \frac{\xi}{1+\xi} n_{ij} n_{kl} \Delta \hat{e}_{kl} - \frac{1}{2} \frac{\xi}{1+\xi} \frac{E_{\tan}}{E_{\sec}} \frac{\hat{s}_{ij}}{\varphi} \right], \tag{4.5}$$

where

$$\xi = \Delta \hat{x}_1 \frac{\varphi}{E_{\tan}} \frac{Q}{m_s}, \qquad Q = \frac{\hat{\gamma}_0 \sqrt{\mu\rho}}{\tau_f^2} G,$$
$$E_{\tan} = \frac{\partial(\tau/\mu)}{\partial(\dot{\gamma}^{\mathrm{p}}/\dot{\gamma}_0)} \qquad E_{\sec} = \frac{\tau/\mu}{\dot{\gamma}^{\mathrm{p}}/\dot{\gamma}_0}. \tag{4.6}$$

Here $\Delta \hat{s}_{ij}$ and $\Delta \hat{e}_{ij}$ are the incremental changes in deviatoric stress and strain for an incremental change in position $\Delta \hat{x}_1$ along a pathline, and $\varphi$ is a linear-interpolation parameter with value between 0 and 1 (cf. Peirce *et al.*[14]). The parameter $Q$ arises naturally in the course of normalization. It is a combination of material parameters and the overall dynamic energy release rate $G$. Like the parameter $P$ used in [3], $Q$ can be interpreted as a measure of load intensity and it plays a central role in characterizing the steady-crack-growth process.

It is noted that the integration formula (4.5) reduces to the standard Euler formula when $\varphi = 0$, and that it corresponds to elastic material response when $Q = 0$ but $\varphi \neq 0$. As $Q$ approaches infinity, the response represented by (4.5) approaches the case of rate-independent, elastic-perfectly plastic material response.

Equation (4.5) applies to regions in which the response is represented by either of the two forms of the plastic-strain-rate equation, that is, either (2.1) or (2.2). It must be kept in mind that for a given $\Delta \hat{e}_{ij}$, the change in state of stress at a material point resulting from application of (4.5) may result in a change of operative constitutive equation at that point. This matter is handled by incorporating the ideas of Rice and Tracey[15]. For each increment $\Delta \hat{x}_1$, a check is made to see if a strain increment $M\Delta \hat{e}_{ij}$ with $0 < M < 1$ will carry the stress state to a boundary of the current response regime, e.g. to $\tau_t$ or $\tau_y$. If not, (4.5) is applied directly. Otherwise, the final stress state is computed as resulting from separate strain increments $M\Delta \hat{e}_{ij}$ and $(1 - M)\Delta \hat{e}_{ij}$, with each based on the appropriate form of $F(\tau)$ in (4.5).

## 5. RESULTS

A typical result showing the boundaries of the different regimes of rate-dependent plastic flow is shown in Fig. 2 for $\nu = 0.3c_s$, $Q = 20$, $\nu = 0.3$ and temperature of 300 K. The inner contour is the locus of points for which the effective plastic-shear-strain rate is $\hat{\gamma}_t$, and the outer contour is the locus of points for which the effective plastic strain rate is 1 $s^{-1}$. The inner contour is determined almost completely by the value of $Q$ but the outer boundary depends on the prevailing temperature.

The energy dissipated in each portion of the active plastic zone was determined from the finite-element solution by means of numerical integration of the area integral term in (3.4). It was found that the energy dissipated per unit crack advance in the inner (high-strain-rate) part of the active plastic zone is usually greater than 90% of $G$. For the situation depicted in Fig. 2, the percentage is actually 94% of $G$. This observation provides justification for the approx-

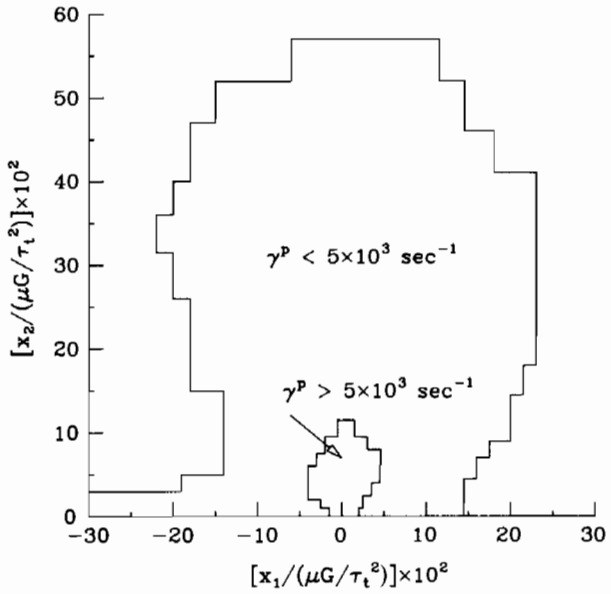


Fig. 2. The active crack-tip plastic zone for the particular case of $m_\gamma = 0.3$, $Q = 20$ and $\nu = 0.3$, showing the inner high-strain-rate region and the outer low-to-moderate strain-rate region.

imation made in [3], according to which the energy dissipated in the outer part of the active plastic zone was simply neglected in estimating the total energy dissipated through plastic flow. It also supports the suggestion made above that the precise definition of $\tau_y$ is immaterial.

Particular insight into the phenomenon of high-strain-rate crack growth was gained in [3] by examining the dependence of the ratio $G_{\text{tip}}/G$ on $Q$ (in [3], a parameter called $P$ which is proportional to $Q$ was used). Consequently, the same dependence has been examined for the finite-element solution as well. For purposes of direct comparison, the portion of the energy locked in the wake as residual elastic energy has also been ignored in the interpretation of the numerical results. The results of the comparison are shown in Fig. 3, where the continuous curves represent the expression in eqn (6.3) in [3] with $Q$ set equal to $3P$. It is evident that the agreement diminishes in quality as $Q$ increases, for any given value of $m$. This matter was pursued by examining the computed stress fields around the crack tip, rather than considering only the global energy quantities. While space does not permit graphical representation of these stress distributions here, the general observation is that the departure of the approximate solution of [3] and the numerical finite solution corresponds to substantial deviations of the near-tip stress distribution from the elastic distribution. Recall that it was assumed in [3] that the near-tip distribution was exactly the elastic stress distribution, and the ratio $G_{\text{tip}}/G$ was estimated on this basis.

The energy rate balance (3.4) was deduced in [3] by application of a path-independent integral introduced by Hutchinson[16] for steady quasistatic crack growth and by Willis[17] for steady dynamic growth, namely

$$I = \int_C [(U + T)n_1 - \sigma_{ij}n_j u_{i,1}]\, \mathrm{d}C, \tag{5.1}$$

where $U$ is the stress work density, $T$ is the kinetic energy density, and $C$ is a path encircling the tip of a crack growing steadily in the $x_1$ direction. The value of $I$ is the same for all crack-tip contours $C$ which start on one traction-free crack face and end on the opposite traction-free crack face. If it is recognized that $I = G_{\text{tip}}$ and if the normalization of field quantities in (4.1) is introduced, then it can be shown that

$$\frac{G_{\text{tip}}}{G} = \int_C [(\hat{U} + \hat{T})\, n_1 - \hat{\sigma}_{ij}n_j\hat{u}_{i,1}]\, \mathrm{d}\hat{C}. \tag{5.2}$$

The value of the integral (5.2) was considered for 12 integration paths around the crack tip for

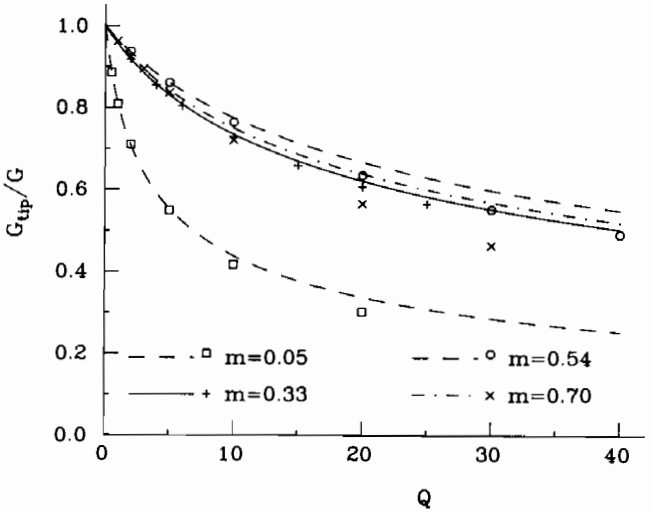


Fig. 3. The ratio of the crack-tip energy release rate $G_{\text{tip}}$ to the rate of energy flow into the crack-tip region $G$ *vs* $Q$, for several values of crack-tip speed. The curves are the result of the approximate analysis in [3] whereas the discrete points are the result of numerical computation based on the same model.

each numerical solution. The innermost path passed through the centers of just the 8 finite elements nearest the tip, and each successive path was formed by moving the previous path outward from the tip one element spacing. It was found that the average value of $G_{tip}/G$ for the 12 paths for each numerical solution differed from the value plotted in Fig. 3 by only 1–2% in most cases, and the difference was never greater than 4%. The difference may be due in part to the elastic energy stored in the wake of the active plastic zone, which is included in (5.2) but not in the estimate appearing in Fig. 3. In any case, the general consistency contributed to confidence in the adequacy of the numerical procedure.

Finally, the application of the theory in [3] to the growth of a macroscopic cleavage crack in mild steel is reviewed in light of the computational results. Suppose that the criterion for the crack to run under steady-state conditions is

$$G_{tip} = G^c_{tip}. \tag{5.3}$$

The critical energy release rate $G^c_{tip}$ represents the energy per unit crack extension absorbed by the fracture processes and not otherwise accounted for by the continuum analysis. For simplicity, $G^c_{tip}$ is viewed as a material constant, independent of crack speed $v$ or temperature. If the definition of $Q$ is recalled from (4.6), the growth criterion (5.3) may be rewritten as

$$\frac{G^c_{tip}}{G} = \frac{Q_c}{Q}, \tag{5.4}$$

where $Q_c = \dot{\gamma}_0\sqrt{\mu\rho}G^c_{tip}/\tau_t^2$. Note from (3.6) that $Q_c \approx 3P_c$, with the difference being slightly temperature dependent due to the second term in brackets in (3.6). On the basis of material properties data given by Frost and Ashby[5] and Campbell and Ferguson[4], the estimate $G^c_{tip} = 1.73 \times 10^3$ N/m was deduced in [3]. Typical values of $Q_c$ were found to be 4.84, 9.57 and 18.56 for temperatures of 100, 200 and 300 K, respectively.

In the coordinates of Fig. 3, the relationship (5.4) represents a hyperbola. If this hyperbola is superimposed onto Fig. 3, then the intersection of this hyperbola for a particular value of $Q_c$ or temperature with the corresponding curve on that figure yields a combination of the quantities $G^c_{tip}/G$, $Q$, and $m$ for which the steady-growth condition (5.3) is satisfied. This result of the computational procedure may then be compared to the result (3.5) based on the approximate analysis of [3]. This comparison is made in Fig. 4, which shows three curves of $G_s/$

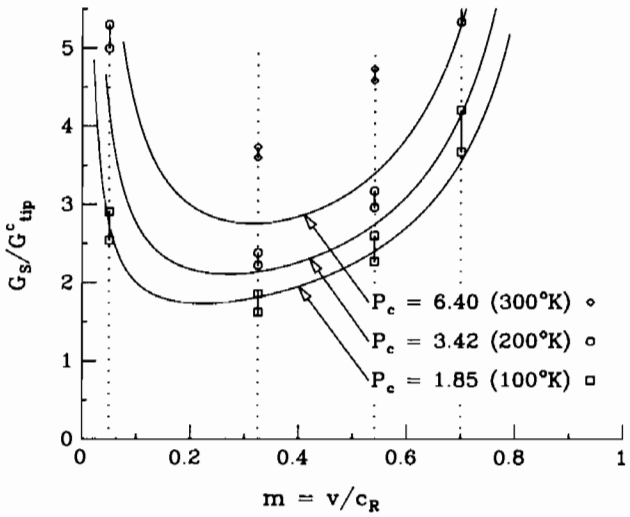


Fig. 4. The ratio of remote crack-driving force $G_s$ to the crack-tip energy release rate $G^c_{tip}$ *vs* crack-tip speed for steady growth for three values of the characterizing parameter $P_c$. The curves are from [3] whereas the discrete points are the result of numerical computations based on the same model. Material parameters typical of mild steel were selected, as described in the text.

$G^c_{tip}$ *vs* $m$ for three values of $Q_c$ (or, equivalently, three values of temperature of about 100, 200 and 300 K). The curves correspond to data in Fig. 7 of [3]. The discrete points of Fig. 4 are the values extracted from the numerical procedure. The lower point of each pair follows from the assumption that $Q_c = 3P_c$, while the upper point of each pair follows from independent calculations of $P_c$ and $Q_c$ for the noted temperatures. It is evident that the results of the computational procedure support the earlier results based on an approximate analysis for low temperatures (or low values of $Q_c$). The data show, however, that as the value of $Q_c$ increases to about 20 (or the temperature increases to about 300 K) the approximate analysis of [3] significantly underestimates the amount of plastic dissipation and, consequently, underestimates the level of applied driving force $G$ required to sustain steady growth of the crack.

## 6. CONCLUSIONS

The parameter $Q$, which depends on material parameters and the remote crack-driving force, arises naturally in the formulation of the computational problem in terms of nondimensional quantities. As was suggested in [3], this parameter can be used to characterize the high-strain-rate crack-growth process. Temperature dependence is incorporated entirely through the temperature influence on the various elements of $Q$.

The results of detailed numerical computation support the assumptions underlying the approximate analysis reported in [3] *when $Q$ is sufficiently small*. In this case, the plastic strains are small compared to the elastic strains and the asymptotic near-tip stress distribution provides a reasonable approximation to the actual stress distribution throughout the entire portion of the active plastic zone in which the strain rates are very high. When $Q$ becomes relatively large, the numerical results diverge from the results of the approximation analysis, particularly at very high and very low crack-tip speeds. At the high crack speeds, the divergence seems to be due to the fact that the plastic zone becomes too large for the asymptotic crack-tip field to provide an acceptable approximation to the stress distribution throughout the plastic zone, and the plastic dissipation calculated on the basis of this assumption underestimates the actual dissipation as shown in Fig. 3. At low crack speeds, on the other hand, the divergence seems to be due to the fact that a material particle near the crack tip is subjected to high stress levels for a long enough time for substantial plastic flow to accumulate, thus invalidating the basic assumption of an underlying elastodynamic stress distribution near the crack tip. From experience with crack growth in rate-independent elastic–plastic solids, it is anticipated that the range of validity of the $K_{tip}$-dominated near-tip field vanishes completely as the crack-tip speed $m$ approaches zero.

A nondimensional parameter $\beta$, defined in (3.7) above, was introduced in [3] to provide a measure of whether or not a crack-growth process was indeed a high-strain-rate process. In the present formulation, the parameter is exactly equal to $Q/m_s$. From the data in Fig. 3, it is clear that the approximate analysis, which is based on several assumptions consistent with high-strain-rate response, is accurate for values of $\beta = Q/m_s$ up to about 20 for any crack-tip speed. For values of $\beta$ which exceed 20, the numerical results and the approximate analytical results diverge, especially at the high and low crack speeds. It is noteworthy that the main qualitative feature deduced in [3], namely the elimination of accessible propagation states as $Q_c$ increases, is preserved in the more detailed numerical simulation.

*Acknowledgments*—The work of LBF and PSL was supported by the NSF Materials Research Laboratory at Brown University under Grant No. DMR83-16893 and by the Office of Naval Research under Grant No. N00014-78-C-0051. The work of J.W.H. was supported by the National Science Foundation under Grants DMR83-16979 and MEA82-13925, and by the Division of Applied Sciences at Harvard University.

## REFERENCES

[1] M. L. Wilson, R. H. Hawley and J. Duffy, The effect of loading rate and temperature on fracture initiation in 1020 hot-rolled steel. *Engineering Freacture Mechanics* **13**, 371–385 (1980).

[2] A. N. Stroh, A theory of the fracture of metals. *Advances in Physics* 6, *Philosopical Magazine Supplement*, 418–465 (1957).

[3] L. B. Freund and J. W. Hutchinson, High strain rate crack growth in rate dependent solids. *Journal of the Mechanics and Physics of Solids* **33**, 169–191 (1985).

[4] J. D. Campbell and W. G. Ferguson, The temperature and strain rate dependence of the shear strength of mild steel. *Philosophical Magazine* **21,** 63–82 (1970).
[5] H. J. Frost and M. F. Ashby, *Deformation Mechanism Maps*. Pergamon Press, Oxford (1982).
[6] R. J. Clifton, Dynamic plasticity. *Journal of Applied Mechanics—50th Anniversary Issue* **50,** 941–952 (1983).
[7] J. R. Rice, Mathematical analysis in the mechanics of fracture, in *Fracture: An Advanced Treatise*, Vol. II (H. Liebowtiz, ed.), pp. 191–311. Academic Press (1968).
[8] L. B. Freund, The analysis of elastodynamic crack tip fields, in *Mechanics Today*, Vol. 3 (S. Nemat-Nasser, ed.), pp. 55–91. Pergamon Press (1976).
[9] K. K. Lo, Dynamic crack tip fields in rate sensitive solids. *Journal of the Mechanics and Physics of Solids* **31,** 287–305 (1983).
[10] B. Brickstad, A viscoplastic analysis of rapid crack propagation experiments in steel. *Journal of the Mechanics and Physics of Solids* **31,** 307–327 (1983).
[11] R. H. Dean and J. W. Hutchinson, Quasistatic steady crack growth in small scale yielding, in *Fracture Mechanics. ASTM STP* **700,** 383–405 (1980).
[12] P. S. Lam and L. B. Freund, Analysis of dynamic growth of a tensile crack in an elastic–plastic material. *Journal of the Mechanics and Physics of Solids* **33,** 153–167 (1985).
[13] D. M. Parks, P. S. Lam and R. M. McMeeking, Some effects of inelastic constitutive models on crack tip fields in steady quasistatic growth, in *Advances in Fracture Research*, Vol. 5 (D. Francois, ed.), pp. 2607–2614. Pergamon Press (1981).
[14] D. Peirce, C. F. Shih and A. Needleman, A tangent modulus method for rate dependent solids. *Computers and Structures* **18,** 875–887 (1984).
[15] J. R. Rice and D. M. Tracey, Computational fracture mechanics, in *Numerical and Computer Methods in Structural Mechanics* (S. J. Fenves *et al.*, eds.), pp. 585–623. Academic Press (1973).
[16] J. W. Hutchinson, On steady quasistatic crack growth, Harvard University Report, Division of Applied Sciences Rept. No. DEAP S-8 (1974).
[17] J. R. Willis, Equations of motion for propagating cracks, in *The Mechanics and Physics of Fracture*, pp. 57–67. The Metals Society (1975).